Pair distribution functions of a binary Yukawa mixture and their asymptotic behavior

Christian Tutschka,[1] Gerhard Kahl,[1] and Giorgio Pastore[2]
[1]*Institut für Theoretische Physik and CMS, TU Wien, Wiedner Hauptstraße 8-10, A-1040 Wien, Austria*
[2]*INFM and Dipartimento di Fisica Teorica, Università di Trieste, Strada Costiera 11, I-34014, Trieste, Italy*
(Received 6 February 2001; published 25 May 2001)

Based on an analytic solution of the mean spherical model for a binary hard sphere Yukawa mixture, we have examined the pair distribution functions $g_{ij}(r)$, focusing, in particular, on two aspects: (i) We present two complementary methods to compute the $g_{ij}(r)$ accurately and efficiently over the entire r range. (ii) The poles of the Laplace transforms of the pair distribution functions in the left half of the complex plane close to the origin determine the universal asymptotic behavior of the $g_{ij}(r)$. Although the meaning of the role of the subsequent poles—which typically are arranged in two branches—is not yet completely clear, there are strong indications that the distribution pattern of the poles is related to the thermodynamic state of the system.

DOI: 10.1103/PhysRevE.63.061110 PACS number(s): 61.20.Gy, 61.20.Ne, 05.20.−y, 02.30.−f

I. INTRODUCTION

A series of model systems still plays, despite its simplicity, an important role in the theory of classical fluids: the pair interactions of the particles are characterized, throughout, by a hard core part, at contact adding an attractive (or repulsive) tail. These systems are commonly referred to—in order of increasing complexity—as hard spheres (HS's), adhesive HS's, charged HS's, and HS's with a Yukawa tail (HSY). Characteristic of these systems is the fact that their structural and thermodynamic properties can be obtained from the solution of the Ornstein-Zernike (OZ) equation—along with a suitable closure relation—to a large extent *analytically*. These systems were studied in the late 1960s and 1970s, but, still, considerable effort is being dedicated to research activities of these systems; of course, meanwhile, the ideas that are pursued have changed to a higher level of complexity.

There are several reasons why these analytically solvable model systems are still that attractive, and in the following a few of them we list: (i) The interatomic potentials of some colloidal suspensions can be modeled quite accurately by such hard core interactions [1]. (ii) It is certainly more convenient to start the development of new theoretical methods or basic investigations from simple model systems, where at least for the structural and thermodynamic properties of the uniform fluid analytic expressions are available; three recent examples of such investigations are the extension of multicomponent concepts to the polydisperse case [2,3] and the development of the fundamental measure theory [4] or of the self-consistent OZ approximation [5]. These developments were started, throughout, for such analytically solvable models. (iii) Despite the simplicity of their interactions, such systems show phenomena which are *qualitatively* similar to systems with more realistic potentials.

The present paper is dedicated to a detailed analysis of the structural properties of a binary HSY mixture; we address aspects of the above mentioned items (ii) and (iii). Among the series of model systems mentioned before, the HSY interaction represents undoubtedly the most general potential, since it covers—via special limiting prescriptions—the remaining three cases. The properties of a HSY mixture are given within the mean spherical model (MSM) to a large extent by analytical expressions only. While the solution of the MSM in terms of the direct correlation functions and the calculation of the thermodynamic properties have been discussed (see Ref. [6] and subsequent papers), in the present paper we focus on a closer analysis of the pair distribution functions (PDF's) $g_{ij}(r)$ of a binary HSY mixture: first, we present two complementary semianalytic methods to compute the pair distribution functions; based on these representations of $g_{ij}(r)$, in a subsequent step we investigate the asymptotic behavior of these functions and the distribution of the poles of the $\hat{g}_{ij}(t)$, the Laplace transforms of the $[rg_{ij}(r)]$, in the left half (LH) of the complex t plane.

Additional motivation for our investigations on HSY systems comes from a more *methodological* aspect. HS and HSY systems play an important role as reference systems in thermodynamic perturbation theories. In this context, the HSY system can be used in at least three ways: (i) as a reference system for potentials with long range interactions, (ii) as an improved parametrization of a HS system (as for instance in the framework of the generalized mean spherical model [7]), and (iii) as an exact benchmark for numerical solutions of integral equations. In all cases an accurate and efficient calculation of the PDF's in the entire r range is required, avoiding, at the same time, time-consuming numerical Fourier transforms and numerical inaccuracies introduced by discontinuities of the correlation functions at contact. This aspect is covered by the first goal of this paper: we present a generalization of two methods [known in literature as the shell representation (SR) and the asymptotic representation (AR); for a brief historic review, see Ref. [8]] to the case of a HSY system, which together form a reliable tool for the calculation of the PDF's. The methods are complementary in the sense that they allow a computation of PDF's in the entire r range: the SR is more suitable for distances from contact up to intermediate r values, while in more distant regions (where the SR becomes conceptually tedious and numerically inaccurate) the AR becomes more appropriate. The overlap region is located around five times the respective HS diameter.

Both approaches are based on the availability of analytic expressions for $\hat{g}_{ij}(t)$ which can be extracted from an ana-

lytic solution of the MSM for the HSY system: they can be derived via the Wiener-Hopf (WH) factorization of the OZ equations for this system. In the SR the Laplace transform back into r space is done shell by shell, a shell being defined via $\{r|r \geqslant \xi\}$ and ξ being a linear combination of the two HS diameters. The method is particularly useful for small and intermediate distances, where the number of terms (which is increasing rapidly with increasing r) is still reasonable. The AR is based on an application of the residue theorem; the PDF's can be represented as a series of exponentially decaying or damped oscillating functions. The attractive feature of this method is that the functional form of the terms in this series is always the same, and that hence each additional term added to the above expansion requires a fixed amount of resources. This representation gives results with high accuracy for intermediate r values up to infinity. In this paper we provide all expressions required to implement both the SR and AR for a binary HSY system (with one Yukawa tail). The paper contains, furthermore, a discussion of the numerical validity and reliability of the combined methods.

From the structure of the AR it is obvious that the poles of the $\hat{g}_{ij}(t)$ closest to the origin determine the asymptotic behavior of the PDF's. Lebowitz and Percus [9] were (probably) the first to discover that for large distances a PDF is characterized by an exponential decay or by an exponentially damped oscillatory behavior. Martynov [10] found that even in a more component system there is only one single exponential decay length and only one oscillatory wavelength for *all* partial PDF's. In subsequent work, Evans and Henderson (with their respective co-workers) discussed this *universal asymptotic behavior* in a more systematic and detailed way [11–16]. They focused their interest, in particular, on the two poles located closest to the origin [17], one of them being real, the other a pair of complex conjugates. The fact that either the real pole is closer to the origin and the complex conjugate poles further away, or vice versa, leads to a fundamentally different long range behavior of the PDF's; the corresponding two thermodynamic states of the system are separated in the phase diagram by the so-called Fisher-Widom (FW) line [18]. This investigation was also extended to study the influence of this effect on density profiles (e.g., Ref. [11]). In this paper we resume this analysis for our binary HSY mixture; in addition, we go one step further by extending the search for poles to a larger subarea of the LH of the complex t plane. The poles arrange in two branches plus two (independent) poles on the real axis, apart from the trivial double pole at the origin. We were able to identify in a qualitative way how these poles vary as we modify the system parameters. While these additional poles do not contribute to the asymptotic behavior of the PDF's, there are strong indications that the information contained in such a pole distribution is related to the thermodynamic state the system is in.

The paper is organized as follows: in Sec. II we briefly review the MSM for the HSY mixture and present the SR and the AR (along with the expressions required for the actual calculations); this section is concluded with a discussion of the accuracy and efficiency of the two representations. In Sec. III we discuss the universal asymptotic behavior of the PDF's and the topology of the pole distribution of $\hat{g}_{ij}(t)$. The paper closes with concluding remarks.

II. REPRESENTATIONS OF THE PAIR DISTRIBUTION FUNCTIONS

A. Analytic solution of the MSM for a binary HSY mixture

The structure of a binary HSY mixture is obtained from the OZ relation

$$h_{ij}(r) = c_{ij}(r) + \sum_k \rho_k \int h_{ik}(\mathbf{r}') c_{kj}(|\mathbf{r} - \mathbf{r}'|) d^3 r', \qquad i,j,k = 1,2 \tag{1}$$

along with the hard core MSM closure relations

$$h_{ij}(r) = -1, \quad r < R_{ij}, \tag{2}$$

$$c_{ij}(r) = \frac{1}{r} K_{ij} \exp[-z(r - R_{ij})] = -\beta \Phi_{ij}(r), \quad r > R_{ij}. \tag{3}$$

$h_{ij}(r)$ and $c_{ij}(r)$ are the total and direct correlation functions, and $\Phi_{ij}(r)$ are Yukawa potentials. R_i $(=R_{ii})$ are the core radii of species i, $R_{12} = (R_1 + R_2)/2$, K_{ij} are the contact values, and z is the screening length. $\beta = 1/(k_B T)$, k_B being the usual Boltzmann constant and T the temperature. ρ stands for the total number density, c_i is the concentration of species i, and $\rho_i = \rho c_i$ are the partial number densities. We also introduce the partial (η_i) and total (η) packing fractions:

$$\eta_1 = \frac{\pi}{6} \rho_1, \quad \eta_2 = \frac{\pi}{6} \rho_2, \quad \eta = \eta_1 R_1^3 + \eta_2 R_2^3. \tag{4}$$

One should point out here that the MSM can also be solved for the more general case where $\Phi_{ij}(r)$ in Eq. (3) are superpositions of k Yukawa tails, each of them characterized by contact values $K_{ij}^{(n)}$ and screening lengths z_n, $k = 1, \ldots, n$ [6,19]. This extended concept can also be used in the SR and AR (introduced in Sec. II B), leading, however, to expressions that are thus substantially more complex than those for the case of one Yukawa tail.

The MSM for a HSY system may be solved either by using the Laplace transform technique introduced by Wertheim [20] or by using the WH factorization technique introduced by Baxter [21]. In this paper we use the latter, following the derivation of Blum and Høye [6]: to this end, factor functions, $Q_{ij}(r)$, are defined; for the HSY case they are found to be [6]

$$Q_{ij}(r) = Q_{ij}^0(r) + D_{ij} \exp[-zr], \tag{5}$$

$$Q_{ij}^{0}(r)=\begin{cases}\frac{1}{2}q_{ij}''(r-R_{ij})^2+q_{ij}'(r-R_{ij})+C_{ij}\{\exp[-zr]-\exp[-zR_{ij}]\}, & \lambda_{ji}\leqslant r<R_{ij}\\ 0, \quad R_{ij}\leqslant r\end{cases} \tag{6}$$

with $\lambda_{ij}=(R_i-R_j)/2$. Note that the $Q_{ij}(r)$ are not symmetric, i.e., $Q_{ij}(r)\neq Q_{ji}(r)$ [21], and that different parametrizations for the $Q_{ij}(r)$ are used in Refs. [21,6,22]. As worked out in detail by Blum and Høye [6] the unknown coefficients q_{ij}', q_{ij}'', C_{ij}, and D_{ij} are determined from five sets of coupled nonlinear equations. Among the multiple solutions of this system of equations only one corresponds to a nondiverging solution of the original equations (1)–(3) [6,22]. Once we have obtained this solution we can determine $Q_{ij}(r)$ and all the structural and thermodynamic properties of the HSY system for the MSM.

We then define the functions $\hat{Q}_{ij}(t)$ as

$$\hat{Q}_{ij}(t)=\int_{\lambda_{ji}}^{\infty}ds\,e^{-st}Q_{ij}(s), \tag{7}$$

which may be cast into the form

$$\hat{Q}_{ij}(t)=\frac{\exp(-tR_{ij})}{2t^3(t+z)}\{f_{ij}^{0}(t)+\exp(tR_i)[f_{ij}^{1}(t)-f_{ij}^{0}(t)]\}, \tag{8}$$

where t is henceforward a *complex* variable. The coefficient functions $f_{ij}^{0}(t)$ and $f_{ij}^{1}(t)$ are polynomials in t and are compiled in the Appendix. Some of the expressions presented there require symmetry relations which hold between the q_{ij}' and q_{ij}'' [6]. Furthermore, as shown in Ref. [6], the following expressions for $\hat{g}_{ij}(t)$, i.e., the Laplace transforms of the $[rg_{ij}(r)]$, can be obtained from the WH equations:

$$\hat{g}_{11}(t)=-\frac{1}{4\pi t^2(t+z)}\frac{1}{D(t)}\{\exp(-tR_1)f_{11}^{0}(t)\times[1-\rho_2\hat{Q}_{22}(t)]+\rho_2\exp(-tR_{12})f_{12}^{0}(t)\hat{Q}_{21}(t)\}, \tag{9}$$

$$\hat{g}_{12}(t)=-\frac{1}{4\pi t^2(t+z)}\frac{1}{D(t)}\{\exp(-tR_{12})f_{12}^{0}(t)\times[1-\rho_1\hat{Q}_{11}(t)]+\rho_1\exp(-tR_1)f_{11}^{0}(t)\hat{Q}_{12}(t)\}, \tag{10}$$

$$\hat{g}_{22}(t)=-\frac{1}{4\pi t^2(t+z)}\frac{1}{D(t)}\{\exp(-tR_2)f_{22}^{0}(t)\times[1-\rho_1\hat{Q}_{11}(t)]+\rho_1\exp(-tR_{12})f_{21}^{0}(t)\hat{Q}_{12}(t)\}, \tag{11}$$

with

$$D(t)=[1-\rho_1\hat{Q}_{11}(t)][1-\rho_2\hat{Q}_{22}(t)]-\rho_1\rho_2\hat{Q}_{12}(t)\hat{Q}_{21}(t). \tag{12}$$

We now define the functions $L_i(t)$ $(i=0,\ldots,3)$ and $S(t)$ as follows

$$L_0(t)=\rho_1\rho_2\frac{1}{t^2}[f_{11}^{0}(t)f_{22}^{0}(t)-f_{12}^{0}(t)f_{21}^{0}(t)], \tag{13}$$

$$L_1(t)=\rho_2\frac{1}{t^2}\{2f_{22}^{0}(t)t^3(t+z)-\rho_1[f_{11}^{1}(t)f_{22}^{0}(t)-f_{12}^{1}(t)f_{21}^{0}(t)]\}+L_0(t), \tag{14}$$

$$L_2(t)=\rho_1\frac{1}{t^2}\{2f_{11}^{0}(t)t^3(t+z)-\rho_2[f_{22}^{1}(t)f_{11}^{0}(t)-f_{21}^{1}(t)f_{12}^{0}(t)]\}+L_0(t), \tag{15}$$

$$L_3(t)=\frac{1}{2\pi}\frac{1}{t^3}\Big\{-t^3(t+z)[f_{12}^{0}(t)+f_{21}^{0}(t)]+\frac{1}{2}\rho_1[f_{11}^{1}(t)f_{12}^{0}(t)-f_{11}^{0}(t)f_{12}^{1}(t)]+\frac{1}{2}\rho_2[f_{22}^{1}(t)f_{21}^{0}(t)-f_{22}^{0}(t)f_{21}^{1}(t)]\Big\}, \tag{16}$$

$$S(t)=\frac{1}{t^2}\{4t^6(t+z)^2-2t^3(t+z)[\rho_1f_{11}^{1}(t)+\rho_2f_{22}^{1}(t)]+\rho_1\rho_2[f_{11}^{1}(t)f_{22}^{1}(t)-f_{12}^{1}(t)f_{21}^{1}(t)]\}+L_1(t)+L_2(t)-L_0(t). \tag{17}$$

which—despite the prefactors t^{-n}—turn out to be *polynomials* in t. Here, for the HSY case, the $L_i(t)$ $(i=0,\ldots,3)$ are polynomials of orders 2, 4, 4, and 3, and $S(t)$ is of order 6. Throughout they are higher by an order of 2 than the corresponding polynomials of the HS case [8]. Further, for a HSY system the polynomials are considerably more complex: we have therefore shifted the explicit and rather lengthy expressions for the $L_i(t)$'s and $S(t)$ as polynomials in t to the Appendix.

With definitions (13)–(17), we simplify expressions (9)–(11), and finally arrive at

$$\hat{g}_{11}(t)=\frac{t[L_0(t)-L_2(t)\exp(tR_2)]}{12\eta_1D(t)}=\frac{N_{11}(t)}{D(t)}, \tag{18}$$

$$\hat{g}_{12}(t)=\frac{t^2L_3(t)\exp(tR_{12})}{D(t)}=\frac{N_{12}(t)}{D(t)}, \tag{19}$$

$$\hat{g}_{22}(t)=\frac{t[L_0(t)-L_1(t)\exp(tR_1)]}{12\eta_2 D(t)}=\frac{N_{22}(t)}{D(t)}, \qquad (20)$$

where we have explicitly symmetrized $\hat{g}_{12}(t)$.

Furthermore, one should mention at this point that a closer look on the *algebraic structure* of $\hat{g}_{ij}(t)$ (obtained from the WH solution route) for the present model reveals that this form is *common* to all the other analytically solvable model systems mentioned above (solved along with a suitable closure relation): $\hat{g}_{ij}(t)$ can indeed be represented in such a form, if $Q_{ij}(r)$ can be expressed in terms of analytic functions. To be more specific, this observation is valid—apart from the HSY system discussed here [6,23]—for HS's [for the Percus-Yevick (PY) equation [24]], for adhesive HS's (both for the PY equation and the MSM [25,3]), and for charged HS's (for the MSM [26]).

To conclude, one must remark that the WH route to solve the OZ equations along with the MSM is only equivalent to the direct solution of the OZ equation, if the function $\Delta(t)=\det[\delta_{ij}-\sqrt{\rho_i\rho_j}\hat{Q}_{ij}(t)]$ has no zeros in the right half (RH) plane of the complex t plane [21]; it is possible to give a local test to detect the presence of zeros in the RH of the t plane [27]. A sufficient condition to find at least one zero there, is given by $\Delta(0)<0$ [21,27].

B. Shell representation

The SR starts from expressions (18)–(20): the common denominator $D(t)$ is rewritten as

$$D(t)=L_0(t)-L_1(t)\exp(tR_1)-L_2(t)\exp(tR_2)+S(t)\exp[t(R_1+R_2)]. \qquad (21)$$

Following the idea of Throop and Bearman [28] (first illustrated for the pure HS case), we expand $1/D(t)$ for sufficiently large $\mathrm{Re}(t)$ in the form

$$\frac{1}{D(t)}=\frac{\exp[-t(R_1+R_2)]}{S(t)}\sum_{n=0}^{\infty}\left[\frac{I(t)}{S(t)}\right]^n, \qquad (22)$$

with

$$I(t)=L_2(t)\exp(-tR_1)+L_1(t)\exp(-tR_2)-L_0(t)\times\exp[-t(R_1+R_2)], \qquad (23)$$

so that we obtain for the PDF's in r space:

$$rg_{11}(r)=\frac{1}{12\eta_1}\sum_{n=0}^{\infty}\frac{1}{2\pi i}\int\frac{t[L_0(t)-L_2(t)\exp(tR_2)]I^n(t)\exp\{t(r-[R_1+R_2])\}}{[S(t)]^{n+1}}dt, \qquad (24)$$

$$rg_{12}(r)=\sum_{n=0}^{\infty}\frac{1}{2\pi i}\int L_3(t)\frac{I^n(t)t^2\exp[t(r-R_{12})]}{[S(t)]^{n+1}}dt, \qquad (25)$$

$$rg_{22}(r)=\frac{1}{12\eta_2}\sum_{n=0}^{\infty}\frac{1}{2\pi i}\int\frac{t[L_0(t)-L_1(t)\exp(tR_1)]I^n(t)\exp\{t(r-[R_1+R_2])\}}{[S(t)]^{n+1}}dt. \qquad (26)$$

The integrations in Eqs. (24)—(26) have to be taken along a line in the RH of the complex t plane, parallel to the imaginary axis and to the right of all the poles of the integrand: these poles are the six roots of $S(t)$, denoted as t_i.

We now start to discuss the case ''11''; the other cases follow similar lines. Expression (24) may be transformed into

$$rg_{11}(r)=\frac{1}{12\eta_1}\sum_{n=0}^{\infty}\frac{1}{2\pi i}\int\frac{1}{[S(t)]^{n+1}}\sum_{\alpha_1,\alpha_2}tQ_{n;\alpha_1\alpha_2}(t)\times\exp\{t[r-(\alpha_1R_1+\alpha_2R_2)]\}dt,$$

$$\alpha_1=1,\ldots,n+1 \quad \alpha_2=n+1-\alpha_1,\ldots,n+1, \qquad (27)$$

$Q_{n;\alpha_1,\alpha_2}(t)$—being products of $L_0(t)$, $L_1(t)$, and $L_2(t)$—are polynomials of order $2[3(n+1)-(\alpha_1+\alpha_2)]$ in t. They are formally identical to the corresponding expressions of the HS case which are listed in the Appendix of Ref. [8].

If r is now either smaller or larger than $(\alpha_1R_1+\alpha_2R_2)$, the integration path parallel to the imaginary axis has to be closed either by a semicircle in the RH or LH of the t plane: (i) In the first case all poles of the integrand will lie outside the area encircled by the integration path; hence the contributions to $g_{11}(r)$ will be zero. (ii) In the second case we have to close the circle in the LH of the complex plane; all poles of the integrand lie within the enclosed area. The value of the integral is then determined by the residues $R^i_{n;\alpha_1\alpha_2}$, given in Eq. (19) of Ref. [8], assuming single multiplicity of all the zeros t_i.

For the second, i.e., the nontrivial case, we introduce the so-called subshell structure: for a given R_1 and R_2, the $[(n+1)(n+4)/2]$ n subshells $S_{n;\alpha_1\alpha_2}$ are defined by

$$S_{n;\alpha_1\alpha_2}=\{r|r\geqslant(\alpha_1R_1+\alpha_2R_2)\},$$

$$1 \leqslant \alpha_1 \leqslant n+1, \quad n+1-\alpha_1 \leqslant \alpha_2 \leqslant n+1. \tag{28}$$

The contribution of each n subshell to $g_{11}(r)$, denoted by $g^{11}_{n;\alpha_1\alpha_2}(r)$, is then given by

$$g^{11}_{n;\alpha_1\alpha_2}(r) = \frac{1}{12\eta_1}\frac{1}{n!}\sum_{i=1}^{6} a_n^i \exp\{t_i[r-(\alpha_1 R_1 + \alpha_2 R_2)]\}\sum_{j=0}^{n} b^{j,i}_{n;\alpha_1\alpha_2}[r-(\alpha_1 R_1+\alpha_2 R_2)],$$

$$^j\alpha_1 = 1,\ldots,n+1, \quad \alpha_2 = n+1-\alpha_1,\ldots,n+1. \tag{29}$$

The first sum is taken over the six roots t_i of $S(t)$. Formally, the expressions for the coefficients a^i and $b^{j,i}_{n;\alpha_1\alpha_2}$ are listed in the Appendix of Ref. [8]. The actual expressions for the case of a HSY system are obtained from these functions by simply replacing the HS polynomials by the HSY polynomials. Finally, summing over all subshells, we arrive at

$$rg_{11}(r) = \sum_{n=0}^{\infty}\sum_{\alpha_1\alpha_2} rg^{11}_{n;\alpha_1\alpha_2}(r)\Theta[r-(\alpha_1 R_1+\alpha_2 R_2)]. \tag{30}$$

Similar argumentations also hold for the other two PDF's, yielding the following expressions for case ''22'':

$$rg_{22}(r) = \frac{1}{12\eta_2}\sum_{n=0}^{\infty}\frac{1}{2\pi i}\int \frac{1}{[S(t)]^{n+1}}\sum_{\alpha_1,\alpha_2} t\tilde{Q}_{n;\alpha_1\alpha_2}(t) \times \exp\{t[r-(\alpha_1 R_1+\alpha_2 R_2)]\}dt,$$

$$\alpha_2 = 1,\ldots,n+1, \quad \alpha_1 = n+1-\alpha_2,\ldots,n+1, \tag{31}$$

$$g^{22}_{n;\alpha_1\alpha_2}(r) = \frac{1}{12\eta_2}\frac{1}{n!}\sum_{i=1}^{6} a_n^i \exp\{t_i[r-(\alpha_1 R_1+\alpha_2 R_2)]\} \times \sum_{j=0}^{n} \tilde{b}^{j,i}_{n;\alpha_1\alpha_2}[r-(\alpha_1 R_1+\alpha_2 R_2)]^j,$$

$$\alpha_2 = 1,\ldots,n+1, \quad \alpha_1 = n+1-\alpha_2,\ldots,n+1, \tag{32}$$

$$rg_{22}(r) = \sum_{n=0}^{\infty}\sum_{\alpha_1\alpha_2} rg^{22}_{n;\alpha_1\alpha_2}(r)\Theta[r-(\alpha_1 R_1+\alpha_2 R_2)]. \tag{33}$$

Finally, for case ''12,''

$$rg_{12}(r) = \sum_{n=0}^{\infty}\frac{1}{2\pi i}\int \frac{1}{[S(t)]^{n+1}}\sum_{\alpha_1,\alpha_2} tu(t)\overline{Q}_{n;\alpha_1\alpha_2}(t) \times \exp\{t[r-(\alpha_1 R_1+\alpha_2 R_2)/2]\}dt, \tag{34}$$

$$g^{12}_{n;\alpha_1\alpha_2}(r) = \frac{1}{n!}\sum_{i=1}^{4} a_n^i \exp\{t_i[r-(\alpha_1 R_1+\alpha_2 R_2)/2]\} \times \sum_{j=0}^{n} \overline{b}^{j,i}_{n;\alpha_1\alpha_2}[r-(\alpha_1 R_1+\alpha_2 R_2)/2]^j$$

$$\alpha_1 = 1,\ldots,2n+1(2), \quad \alpha_2 = 2n+2-\alpha_1,\ldots,2n+1 \ \ (2), \tag{35}$$

$$rg_{12}(r) = \sum_{n=0}^{\infty}\sum_{\alpha_1\alpha_2} rg^{12}_{n;\alpha_1\alpha_2}(r)\Theta[r-(\alpha_1 R_1+\alpha_2 R_2)], \tag{36}$$

$$u(t) = tL_3(t). \tag{37}$$

Again $\tilde{Q}_{n;\alpha_1\alpha_2}(t)$ and $\overline{Q}_{n;\alpha_1\alpha_2}(t)$ (as well as $\tilde{b}^{j,i}_{n;\alpha_1\alpha_2}$ and $\overline{b}^{j,i}_{n;\alpha_1\alpha_2}$) are formally identical to those of the HS case and are listed in the Appendix of Ref. [8]: the HSY expressions are obtained by replacing the HS polynomials $L_i(t)$ $(i=0,\ldots,3)$ and $S(t)$ by the corresponding polynomials in the HSY case [Eqs. (13)–(17)]. Everything which was told in Ref. [8] for the HS case about the subshell structure (which is imposed by the values of R_1 and R_2) and the resulting limits of validity of this method [cf. Eqs. (24) and (25) of Ref. [8]] also holds for the HSY case of the present paper.

C. Asymptotic representation

In the AR we start again from Eqs. (18)–(20), and we obtain the PDF's in r space via an inverse Laplace transform, i.e.,

$$rg_{ij}(r) = \frac{1}{2\pi i}\int_{\delta-i\infty}^{\delta+i\infty}\frac{N_{ij}(t)}{D(t)}e^{tr}dt, \tag{38}$$

δ being an arbitrary positive number. For $r<R_{ij}$ we can evaluate integral (38) by using a contour integration in the RH of the complex plane, and we will obtain $g_{ij}(r)=0$. For $r>R_{ij}$ we have to close the contour in the LH plane. Since $D(t)$ has an infinite number of zeros in the LH plane, the contributions of the residues from these poles of $\hat{g}_{ij}(t)$ form a series representation of $rg_{ij}(r)$. The poles of $\hat{g}_{ij}(t)$ have to be determined numerically; we have made—for all the systems investigated—the following observations: (i) There is one pole of *order 2* at $t=0$, contributing the value 1 to the PDF's. (ii) We observe two branches (pairs of complex conjugate values) of *simple poles*; two additional (and independent) poles are located on the real axis. The question of whether further higher order poles are present has not been answered rigorously up to now [29]: Perram and Smith [30] proved, for the one-component case of pure HS's, that all the poles are simple. For a more general system with (possibly) more components, no such proof is available. Our observations were confirmed in Ref. [12,13,15].

Thus we arrive at [assuming single multiplicity of the zeros of $D(t)$]

TABLE I. Parameters of four of the binary HSY mixtures investigated in this study; R_1 is assumed to be 1 in all cases. The partial PDF's $g_{11}(r)$ and the pole distributions of all these systems are shown in the figures.

System	η	c_1	R_2	K_{11}	K_{12}	K_{22}	z
I	0.30	0.65	1.500	1.3947	1.3947	1.8828	2.00
II	0.50	0.75	1.167	0.8333	1.2508	1.8662	1.75
III	0.50	0.25	1.167	0.6897	1.0352	1.5445	2.25
IV	0.40	0.35	1.500	1.1111	1.1111	1.5000	1.75

$$g_{ij}(r)=1+\sum_n h_{ij}^{(n)}(r), \tag{39}$$

where the sum is taken over the roots t_i of $D(t)$ in the LH of the complex t plane. The contributions $h_{ij}^{(n)}$ are given by

$$h_{ij}^{(n)}(r)=\xi\,\mathrm{Re}\left(\frac{N_{ij}(t_n)}{D'(t_n)}\frac{e^{t_n r}}{r}\right), \tag{40}$$

with

$$\xi=\begin{cases}1, & t_n \text{ real}\\ 2, & t_n \text{ complex.}\end{cases} \tag{41}$$

In the following we shall order (and label) the poles t_i according to their respective real parts, pairs of complex conjugate poles count as one. Typical pole distributions will be presented and discussed in Sec. II D.

It is worthwhile to point out once again the remarkable conclusion that one can draw from Eq. (38): the behavior of the PDF's for intermediate and large distances is determined by the poles of the $\hat{g}_{ij}(t)$, i.e., the zeros of the denominator $D(t)$. This denominator is common to all partial PDF's, and so is the pole structure; hence, *all* $g_{ij}(r)$ will show the same asymptotic behavior (independent of the specific potential parameters). Only the amplitude and the phases of the oscillations [which are determined by both $D(t)$ and $N_{ij}(t)$] will be different for the partial PDF's. Presumably the first ones who studied this universal asymptotic behavior (for the one component case) were Lebowitz and Percus [9]; Martynov [10] showed that this effect can even be observed in the multicomponent case, i.e., that the asymptotic behavior of the partial PDF's is determined by one set of poles. Finally, systematic and comprising studies of this effect (including the interrelation with the FW line) and its consequences, for instance, on density profiles, were studied in detail by Evans, Henderson, and their respective co-workers [12–16].

D. Comparison

In the following we present the results for the partial PDF's $g_{11}(r)$ for four selected systems (labeled I–IV; the system parameters are compiled in Table I), and compare results obtained by the SR and AR, including an increasing number of poles (n) in expansion (39). We have chosen n to be 3, 6, and 12, respectively. The PDF's of system I show an exponentially decaying long-range behavior, while the $g_{ij}(r)$'s of systems II–IV are characterized by damped long range oscillations; hence they are located on the opposite side of the FW line (surface) from system I (following the classification of Refs. [12–16]). The respective pole distributions will be discussed in Sec. III (cf. also the figures presented there). Results for g_{11}'s are shown in Fig. 1.

A different asymptotic behavior is clearly visible: in system I [Fig. 1(a)], the first *two* poles (according to the above ordering) are purely real, leading to an asymptotic exponential decay; superimposed are the oscillations induced by the third pole (a pair of complex conjugate values). In systems II–IV [Figs. 1(b)–1(d)] we observe damped long range oscillations that stem from the smallest (complex conjugate) pole, while the contribution from the real pole (which is further away from the origin) is considerably less pronounced. In system III the two poles closest to the origin are pairs of complex conjugate values.

The results confirm observations already presented in Ref. [8]: for short distances the AR fails, even for $n=12$; it fails, in particular, at and near the contact (Gibbs phenomenon). The region, where substantial differences between the SR and AR are observed depends strongly on the system parameters. For this contribution we have studied 36 systems; we can conclude from our observations that the error–on the basis of a six pole expansion–between the SR and AR in the $g_{ij}(r)$'s for distances five times the respective hard core diameter is throughout less than 10^{-3}%; for larger n values this difference decreases drastically.

III. POLE DISTRIBUTION

For the discussion of the pole distribution we have extended the search for t_i to a subarea in the LH of the complex t plane, limiting ourselves to the rectangle $\{-13\leqslant \mathrm{Re}(t)\leqslant 0\}\times\{0\leqslant \mathrm{Im}(t)\leqslant 60\}$, i.e., we discuss only the upper left quarter of the t plane (the lower quarter being symmetric and containing only the complex conjugate values of the t_i's). The poles were computed by solving the transcendental equation $D(t)=0$; note that the determination of the t_i sometimes becomes—depending on the system parameters—a rather delicate task: this is particularly the case when the first pole on the real axis is very close to the origin (e.g., the system is near to a phase separation; see below). Since we determined the poles directly from the explicit expression of $D(t)$ (i.e., what Leote de Carvalho *et al.* [16] called the ''analytic path'') we did not encounter ''spurious poles'' [16] (which stem from numerical convergence problems).

From previous studies we know that in the one compo-

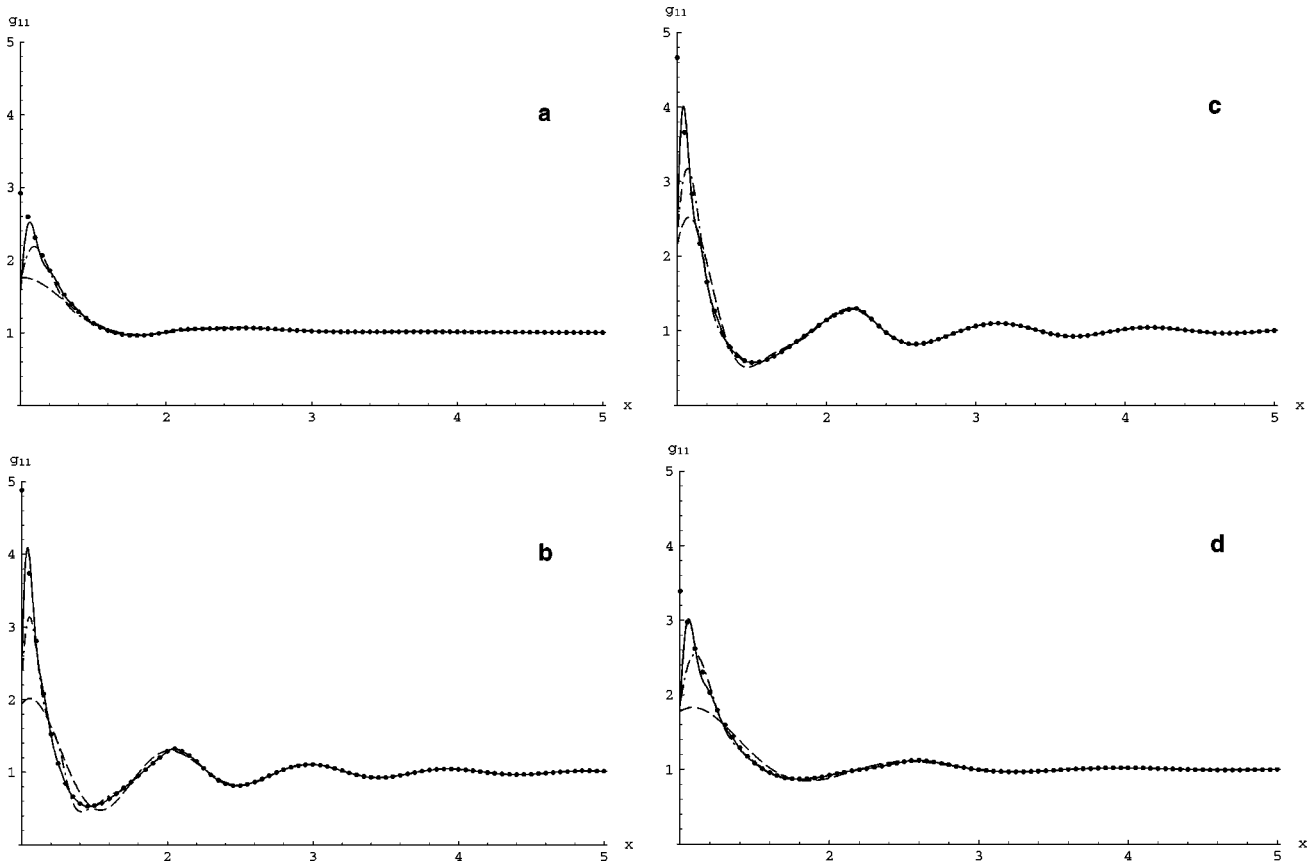

FIG. 1. Partial PDF's $g_{11}(x)$ as functions of $x=r/R_1$ for systems I–IV [(a)–(d); for system parameters see Table I]. •, SR; lines, AR [taking into account n poles in expansion (39): broken line, $n=3$; dot-dashed line, $n=6$; full line, $n=12$].

nent case the poles are arranged in one single branch (cf., for instance, Refs. [12,14,16] for various one component systems). For the PY equation of a binary HS mixture [8] (the only binary system that was investigated in this respect up to now) the poles are located along two branches. Calculations for the ternary HS case (again using the PY equation and the expressions presented in Ref. [31]) showed that also here two branches of poles are found [32]; hence the significance of the number of branches is presently unclear.

The pole distributions of systems I–IV represent archetypes of pole distributions that we have filtered out from our results; these distributions are displayed in Fig. 2. Note that despite the large variety in the parameters of the systems presented here (cf. Table I), the topologies of the two branches of the pole distributions of systems I, III, and IV are astonishingly similar.

A. Universal asymptotic behavior

We come back to the asymptotic behavior of the PDF's. In this subsection we consider only the two (or three) poles closest to the origin; as explained in Sec. II, these poles are exclusively responsible for the asymptotic behavior of the PDF's: the classification in which either the pole closest to the origin is located on the real axis, followed by a pair of complex conjugate poles, or vice versa, decides whether we observe an exponentially decaying or a damped oscillating long range behavior of the PDF's. Systems classified by these criteria lie on different sides of the FW line (on the surface, in the binary case) in the phase diagram. Our study leads to a natural generalization of this classification scheme: we encountered examples where the first *two* poles are located on the real axis (system I), and only the third one represents a pair of conjugate t_i's; or, conversely, the first *two* poles closest to the origin are pairs of complex conjugate values, the third pole being located on the real axis (system III).

B. Topology of the pole distributions

In the case of a binary HSY mixture the t_i (observed in the area defined above) are arranged in two branches. In addition, two poles on the real axis are found; we have observed that these poles are typically much closer to the origin than the single real pole for binary HS's [8]. The role of the poles located further away from the origin is not yet clear: these t_i are certainly irrelevant for the behavior of the PDF's at intermediate distances and for their asymptotic behavior. However, we surmise that the pattern they form is related to the thermodynamic state the system is in. Of course, without a knowledge of the phase diagram, it is not possible to confirm this conjecture.

The systematic variation of the system parameters (density, concentration, and screening length) leads to a clear picture of the respective influence of these quantities on the pole distribution; we summarize our observations in the fol-

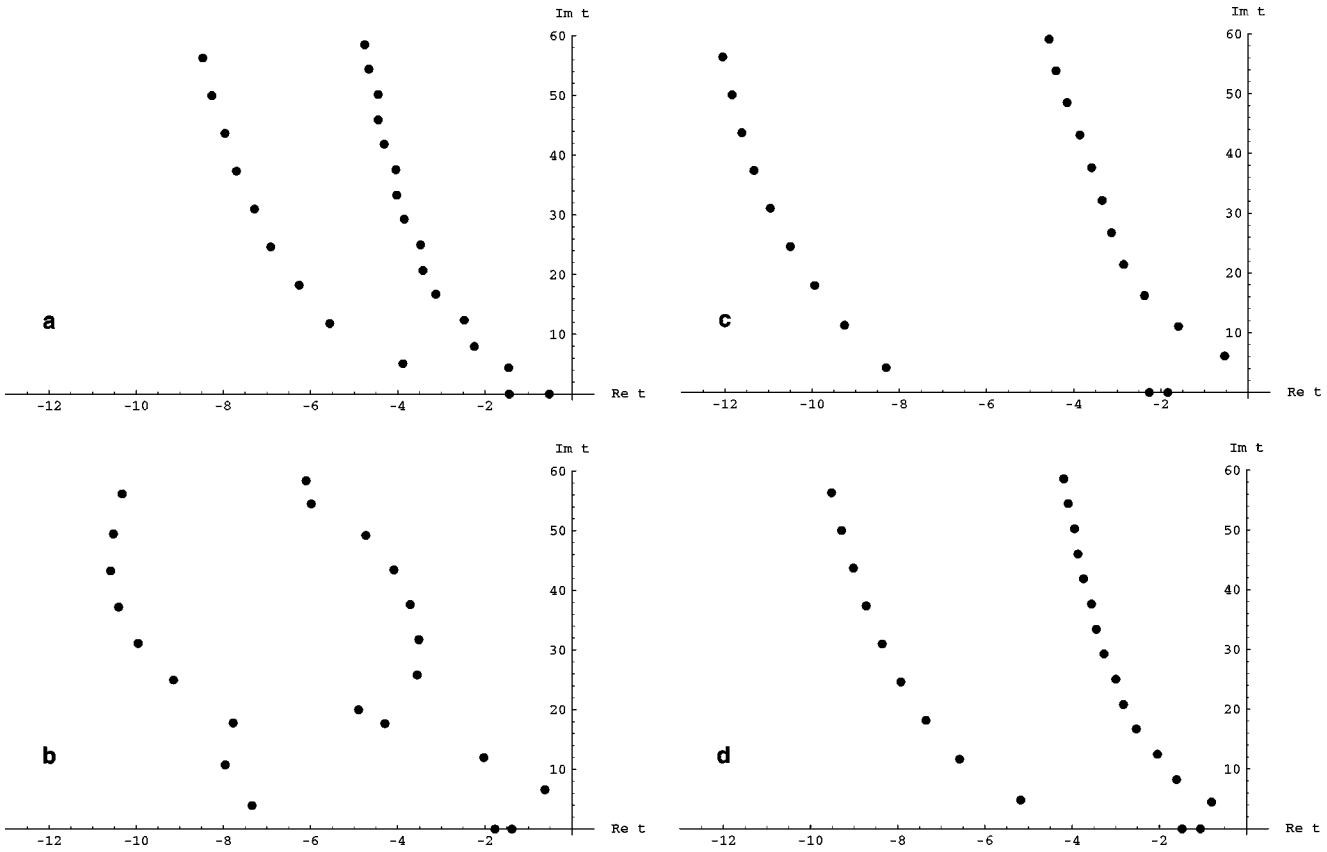

FIG. 2. Distribution of the poles t_l of the $\hat{g}_{ij}(t)$ in a subarea of the upper left quarter of the complex t plane for systems I–IV [(a)–(d)]; the double poles located at the origin have not been marked. The search for t_l has been restricted to $\{-13 \leqslant \mathrm{Re}(t) \leqslant 0\} \times \{0 \leqslant \mathrm{Im}(t) \leqslant 60\}$.

lowing: (i) A large difference between $\rho_1 R_1^3$ and $\rho_2 R_2^3$ leads to clearly separated branches (cf. system III). (ii) Increasing the density ρ shifts the branches toward the imaginary axis of the t plane, but leaves the relative positions of the poles of the branches almost *unaffected*; this shift is easily understood, since the now less negative real parts of the t_i bring about more pronounced oscillations of the PDF's (as it is expected for higher densities). (iii) Finally, a variation of the screening length z shifts the relative position of the two poles on the real axis, leaving the branches of the purely complex conjugate poles nearly *unaffected* (forming hence a robust pattern).

In Fig. 2(a) we show the pole distribution of system I, which—as we know from literature—undergoes a phase separation [22]. The first pole on the real axis is already close to the origin, leading to a very slow exponential decay in the PDF's (an additional hint at the onset of a phase transition); the partial PDF $g_{11}(r)$ for this system is displayed in Fig. 1(a). Figure 2(b) shows the pole distribution of system II; the corresponding PDF $g_{11}(r)$ is presented in Fig. 1(b). The first four poles (two of them are on the real axis, and the others are two pairs of complex conjugates) are clearly separated from the other t_i; these poles are arranged in a pattern where—in contrast to other systems investigated for this study—the two branches are less clearly distinguishable. Certainly, without knowing the phase diagram one is not able to interpret this effect. Figure 2(c) shows the poles of a system where the difference in the $\rho_i R_i^3$ is quite large: here the branches are clearly separated; the branch with the smaller real parts has been pushed to the far end of our observation area. Finally, in Fig. 2(d) we present the pole structure of a system, where the distribution is very similar to the one observed for a binary HS mixture [8] (apart from the additional pole on the real axis).

We are aware that our investigations have left several interesting questions unanswered; we hope to clarify them in a future contribution. There we shall try to relate our observations made for the pole distribution to the thermodynamic state of the system. This can only be done in a comprehensive and a more systematic study: already the phase diagram of a *symmetric* binary mixture (using a subset of system parameters only) is known to be somewhat involved (see, e.g., Ref. [33]), so the general case will be even more complicated.

IV. CONCLUSION

Based on the WH route to solve the MSM for a binary HSY mixture we have presented two complementary representations of the PDF's, the SR and AR. Both dwell on the fact that $\hat{g}_{ij}(t)$, the Laplace transforms of $[rg_{ij}(r)]$, are available in terms of algebraic expressions for this model. The two representations follow from two different expansions of $\hat{g}_{ij}(t)$. The SR is obtained from a shell by shell inversion of these functions, leading to expressions which—with increasing distance r—become extremely tedious and

complex. The AR, being valid for large distances, can only be extended to intermediate and short distances by involving an increasing number of poles of $\hat{g}_{ij}(t)$ in the LH of the complex t plane. However, the two representations are complementary in the sense that together they allow an accurate determination of the PDF's over the *entire r* range; this includes an overlap region (located around five times the respective hard core diameter) where both representations determine the PDF's with a comparable accuracy (errors of less than 10^{-3} % for a six pole AR). We have presented all the expressions that are necessary to implement both representations; they allow a simple extension to the more general case, where the potentials are superpositions of k Yukawa tails.

The determination of the poles of $\hat{g}_{ij}(t)$ required in the AR leads us—as a natural consequence—to a closer analysis of the positions (and distributions) of these poles in the t plane. We have shown that the poles of the binary HSY mixture can be collected in two branches of complex conjugate values and two independent poles on the real axis. We could work out qualitatively how the variation of the system parameters (density, concentration, and screening length) is able to shift the position of the real poles and of the branches. Further, there must be a relation between the pole patterns of the branches and the thermodynamic state of the system: at the level of the PDF's the role of the poles located further away from the imaginary axis is mainly to guarantee the correct contact value (Gibbs phenomenon); however, this means, in particular that—on the level of the thermodynamic properties—these distant poles are responsible for giving the correct equation of state of the system. A detailed analysis of this relation will be reported in a later publication, which will also include investigations of whether a similar analysis is feasible for a system where the required expressions for $\hat{g}_{ij}(t)$ are not available as closed analytic expressions.

ACKNOWLEDGMENTS

This work was supported by the Österreichischer Forschungsfonds (under Project Nos. P13062-TPH and P14371-TPH) and the Wiener Wirtschaftskammer. The authors are indebted to Professor P.T. Cummings (Tennessee) for sending Ref. [34].

APPENDIX

$f_{ij}^0(t)$ and $f_{ij}^1(t)$ used in Sec. II may be written as

$$f_{ij}^0(t)=2\sum_{k=0}^{2} v_{ij}^k t^k, \tag{A1}$$

$$f_{ij}^1(t)=-\sum_{k=1}^{3} w_{ij}^k t^k, \tag{A2}$$

with

$$v_{ij}^0=-zq_{ij}'', \tag{A3}$$

$$v_{ij}^1=-(zq_{ij}'+q_{ij}''), \tag{A4}$$

$$v_{ij}^2=zC_{ij}\exp(-zR_{ij})-q_{ij}', \tag{A5}$$

$$w_{ij}^1=2zR_iq_{ij}'', \tag{A6}$$

$$w_{ij}^2=R_i[2zq_{ij}'-q_{ij}''(zR_i-2)], \tag{A7}$$

$$w_{ij}^3=2C_{ij}[\exp(-zR_{ij})-\exp(-z\lambda_{ji})]-2D_{ij}\exp(-z\lambda_{ji}) + 2q_{ij}'R_i-q_{ij}''R_i^2. \tag{A8}$$

Insertion of Eqs. (A1) and (A2) into the defining expressions of the polynomials $L_i(t)$ $(i=0,\ldots,3)$, and $S(t)$ [Eq. (13)–(17)], and ordering in powers of t, yields the expressions:

$$L_0(t)=4\rho_1\rho_2\sum_{i=0}^{2} l_i^{(0)}t^i, \tag{A9}$$

$$L_1(t)=4\rho_2\sum_{i=0}^{4} l_i^{(1)}t^i+L_0(t), \tag{A10}$$

$$L_2(t)=4\rho_1\sum_{i=0}^{4} l_i^{(2)}t^i+L_0(t), \tag{A11}$$

$$L_3(t)=\sum_{i=0}^{3} l_i^{(3)}t^i, \tag{A12}$$

$$S(t)=\sum_{i=2}^{6} s_it^i+L_1(t)+L_2(t)-L_0(t), \tag{A13}$$

with the coefficients

$$l_m^{(0)}=\sum_{k=m}^{2}(v_{11}^k v_{22}^{2-k}-v_{12}^k v_{21}^{2-k}), \quad m=0,1,2, \tag{A14}$$

$$l_0^{(1)}=\frac{\rho_1}{2}\sum_{k=0}^{1}(v_{22}^k w_{11}^{2-k}-v_{21}^k w_{12}^{k-2}), \tag{A15}$$

$$l_m^{(1)}=zv_{22}^{m-1}+v_{22}^{m-2}+\frac{\rho_1}{2}\sum_{k=m-1}^{2}(v_{22}^k w_{11}^{m+2-k} - v_{21}^k w_{12}^{m+k-2}), \quad m=1,2,3, \tag{A16}$$

$$l_4^{(1)}=v_{22}^2, \tag{A17}$$

$$l_0^{(2)}=\frac{\rho_2}{2}\sum_{k=0}^{1}(v_{11}^k w_{22}^{2-k}-v_{12}^k w_{21}^{k-2}), \tag{A18}$$

$$l_m^{(2)}=zv_{11}^{m-1}+v_{11}^{m-2}+\frac{\rho_2}{2}\sum_{k=m-1}^{2}(v_{11}^k w_{22}^{m+2-k} - v_{12}^k w_{21}^{m+k-2}), \quad m=1,2,3, \tag{A19}$$

$$l_4^{(2)}=v_{11}^2, \tag{A20}$$

$$l_m^{(3)} = 2[z(v_{12}^m + v_{21}^m) + (v_{12}^{m-1} + v_{21}^{m-1})] + \rho_1 \sum_{k=m}^{2} (v_{12}^k w_{11}^{m+3-k} - v_{11}^k w_{12}^{m+3-k}) + \rho_2 \sum_{k=m}^{2} (v_{21}^k w_{22}^{m+3-k} - v_{22}^k w_{21}^{m+3-k}),$$

$$m = 0,1,2, \tag{A21}$$

$$l_3^{(3)} = s(v_{12}^2 + v_{21}^2),$$

$$s_m = 4z\delta_{m,4} + 2\sum_{k=1,2} \rho_k (z w_{kk}^{m-1} + w_{kk}^{m-2}) + \rho_1\rho_2 \times \sum_{k=m-1}^{3} (w_{11}^k w_{22}^{m+2-k} - w_{12}^k w_{21}^{m+2-k}), \tag{A22}$$

$$m = 2,3,4, \tag{A23}$$

$$s_5 = 8z + 2\sum_{k=1,2} \rho_k w_{kk}^3, \tag{A24}$$

$$s_6 = 4. \tag{A25}$$

In the formalism used in this appendix, it may occur in Eqs. (A16), (A19), and (A21), that formally v_{ij}^m with negative m values are required. This is a consequence of our effort to present the above expressions in a very compact form; in fact, $v_{ij}^m = 0$ for negative m.

[1] H. Löwen, Phys. Rep. **237**, 249 (1994).

[2] L. Blum and G. Stell, J. Chem. Phys. **71**, 42 (1979); **72**, 2212 (1980); D. Gazzillo, A. Giacometti, and F. Carsughi, *ibid.* **107**, 10 141 (1997).

[3] C. Tutschka and G. Kahl, J. Chem. Phys. **108**, 9498 (1998).

[4] P. Tarazona and Y. Rosenfeld, in *New Approaches to Problems in Liquid State Theory*, edited by C. Caccamo, J.-P. Hansen, and G. Stell, NATO ASI Series C529 (Kluwer, Dordrecht, 1999), p. 293; Y. Rosenfeld, *ibid.*, p. 303, and references quoted therein.

[5] J. S. Høye, in *New Approaches to Problems in Liquid State Theory* (Ref. [4]), p. 9; D. Pini, G. Stell, and N.B. Wilding, Mol. Phys. **95**, 483 (1998), and references quoted therein.

[6] L. Blum and J. S. Høye, J. Stat. Phys. **19**, 317 (1978).

[7] D. Henderson and L. Blum, Mol. Phys. **32**, 1627 (1976).

[8] G. Kahl and G. Pastore, J. Phys. A **24**, 2995 (1991).

[9] J. L. Lebowitz and J. K. Percus, J. Math. Phys. **4**, 248 (1963).

[10] G. A. Martynov, *Fundamental Theory of Liquids: Method of Distribution Functions* (Hilger, Bristol, 1992).

[11] R. Evans, J. R. Henderson, D. C. Hoyle, A. O. Parry, and Z. A. Sabeur, Mol. Phys. **80**, 755 (1993).

[12] R. Evans, R. J. F. Leote de Carvalho, J. R. Henderson, and D. C. Hoyle, J. Chem. Phys. **100**, 591 (1994).

[13] J. R. Henderson and Z. A. Sabeur, J. Chem. Phys. **97**, 6750 (1992).

[14] R. J. F. Leote de Carvalho, R. Evans, D. C. Hoyle, and J. R. Henderson, J. Phys.: Condens. Matter **6**, 9275 (1994).

[15] R. J. F. Leote de Carvalho and R. Evans, Mol. Phys. **92**, 211 (1997).

[16] R. J. F. Leote de Carvalho, R. Evans, and Y. Rosenfeld, Phys. Rev. E **59**, 1435 (1999).

[17] Instead of searching the poles of $\hat{g}_{ij}(t)$ in the complex t plane, the authors of Refs. [11–16] investigated the Fourier transforms of the PDF's in the complex q plane. From the elementary relation between Fourier and Laplace transforms, it follows that these two sets of poles are related via a rotation by $\pi/2$.

[18] M. E. Fisher and B. Widom, J. Chem. Phys. **50**, 3756 (1969).

[19] E. Arrieta, C. Jędrzejek, and K. N. Marsh, J. Chem. Phys. **95**, 6806 (1991).

[20] M. S. Wertheim, in *The Equilibrium Theory of Classical Fluids*, edited by H. L. Frisch and J. L. Lebowitz (Benjamin, New York, 1964), p. II-268.

[21] R. J. Baxter, J. Chem. Phys. **52**, 4559 (1970).

[22] E. Arrieta, C. Jędrzejek, and K. N. Marsh, J. Chem. Phys. **86**, 3607 (1987).

[23] J. S. Høye and L. Blum, J. Stat. Phys. **16**, 399 (1977).

[24] E. Thiele, J. Chem. Phys. **39**, 474 (1963); M. S. Wertheim, Phys. Rev. Lett. **10**, 321 (1963); J. Math. Phys. **5**, 643 (1964); J. L. Lebowitz, Phys. Rev. **133A**, 895 (1964).

[25] R. J. Baxter, J. Chem. Phys. **49**, 2770 (1968); J. W. Perram and E. R. Smith, Chem. Phys. Lett. **35**, 138 (1975); L. Mier y Terán, E. Corvera, and A. E. González, Phys. Rev. A **39**, 371 (1989).

[26] E. Waisman and J. L. Lebowitz, J. Chem. Phys. **56**, 3086 (1972); **56**, 3093 (1972); R. G. Palmer and J. D. Weeks, *ibid.* **58**, 4171 (1973).

[27] G. Pastore, Mol. Phys. **63**, 731 (1988).

[28] G. Throop and R. J. Bearman, J. Chem. Phys. **42**, 2838 (1965).

[29] We would take the opportunity to point out some misleading passages in Ref. [8]: there we claimed that the pole on the negative real axis ($\tilde{t}$) is a double pole [i.e., $D(\tilde{t}) = D'(\tilde{t}) = 0$ and $D''(\tilde{t}) \neq 0$]. A closer analysis, however, showed that the pole is only a single pole. Numerical results presented in Ref. [8] are—due to the small contribution from that pole—not affected.

[30] J. W. Perram and E. R. Smith, J. Phys. A **13**, 2219 (1980).

[31] E. Paschinger, A. Reiner, and G. Kahl, Mol. Phys. **94**, 743 (1998).

[32] C. Tutschka (unpublished).

[33] N. B. Wilding, F. Schmid, and P. Nielaba, Phys. Rev. E **58**, 2201 (1998).

[34] P. T. Cummings, Ph.D. thesis, University of Melbourne, 1980 (unpublished).